frontiers in Marine Science

BRIEF RESEARCH REPORT
published: 26 November 2020
doi: 10.3389/fmars.2020.584571

Hydrothermal Activity at a Cretaceous Seamount, Canary Archipelago, Caused by Rejuvenated Volcanism

Andreas Klügel[1]*, Heinrich Villinger[1], Miriam Römer[1,2], Norbert Kaul[1], Sebastian Krastel[3], Kai-Frederik Lenz[3] and Paul Wintersteller[1,2]

[1] Fachbereich Geowissenschaften, Universität Bremen, Bremen, Germany, [2] MARUM – Center for Marine Environmental Sciences, Bremen, Germany, [3] Institut für Geowissenschaften, Christian-Albrechts-Universität zu Kiel, Kiel, Germany

Edited by:
Daphne Cuvelier,
Marine and Environmental Sciences
Center (MARE), Portugal

Reviewed by:
Crispin Thomas Stephen Little,
University of Leeds, United Kingdom
Christopher German,
Woods Hole Oceanographic
Institution, United States

***Correspondence:**
Andreas Klügel
akluegel@uni-bremen.de

Specialty section:
This article was submitted to
Deep-Sea Environments and Ecology,
a section of the journal
Frontiers in Marine Science

Received: 17 July 2020
Accepted: 29 October 2020
Published: 26 November 2020

Citation:
Klügel A, Villinger H, Römer M,
Kaul N, Krastel S, Lenz K-F and
Wintersteller P (2020) Hydrothermal
Activity at a Cretaceous Seamount,
Canary Archipelago, Caused by
Rejuvenated Volcanism.
Front. Mar. Sci. 7:584571.
doi: 10.3389/fmars.2020.584571

Our knowledge of venting at intraplate seamounts is limited. Almost nothing is known about past hydrothermal activity at seamounts, because indicators are soon blanketed by sediment. This study provides evidence for temporary hydrothermal circulation at Henry Seamount, a re-activated Cretaceous volcano near El Hierro island, close to the current locus of the Canary Island hotspot. In the summit area at around 3000–3200 m water depth, we found areas with dense coverage by shell fragments from vesicomyid clams, a few living chemosymbiotic bivalves, and evidence for sites of weak fluid venting. Our observations suggest pulses of hydrothermal activity since some thousands or tens of thousands years, which is now waning. We also recovered glassy heterolithologic tephra and dispersed basaltic rock fragments from the summit area. Their freshness suggests eruption during the Pleistocene to Holocene, implying minor rejuvenated volcanism at Henry Seamount probably related to the nearby Canary hotspot. Heat flow values determined on the surrounding seafloor (49 ± 7 mW/m^2) are close to the expected background for conductively cooled 155 Ma old crust; the proximity to the hotspot did not result in elevated basal heat flow. A weak increase in heat flow toward the southwestern seamount flank likely reflects recent local fluid circulation. We propose that hydrothermal circulation at Henry Seamount was, and still is, driven by heat pulses from weak rejuvenated volcanic activity. Our results suggest that even single eruptions at submarine intraplate volcanoes may give rise to ephemeral hydrothermal systems and generate potentially habitable environments.

Keywords: seamount, heatflow, hydrothermal activity, Atlantic, vesicomyid clams, Canary Islands

INTRODUCTION

The seafloor is scattered with hundreds of thousands of volcanic seamounts of >100 m elevation that occur in all parts of the ocean plates (Wessel, 2001; Hillier and Watts, 2007). During their different evolutionary stages, seamounts interact in various ways with the ocean (Staudigel and Clague, 2010). One particular and globally relevant interaction is hydrothermal circulation through seamounts, which extracts significant lithospheric heat and promotes chemical exchange between crust and ocean (Villinger et al., 2002, 2017; Harris et al., 2004; Fisher and Wheat, 2010). At volcanically inactive seamounts, low-temperature hydrothermal circulation can be driven by heat from the cooling lithosphere in conjunction with topographic gradients and basement outcrops (Fisher et al., 2003; Harris et al., 2004; Fisher and Wheat, 2010). At volcanically active seamounts, vigorous hydrothermal activity can be driven by magmatic heat sources at comparatively shallow levels, which is common at arc settings (Butterfield, 2000; de Ronde and Stucker, 2015; Caratori Tontini et al., 2019) but also at some intraplate volcanoes. Examples are very rare, however, and are mostly confined to active systems (Sakai et al., 1987; Staudigel et al., 2004; German et al., 2020) with few exceptions (Medialdea et al., 2017).

Little is known, however, about ephemeral hydrothermal circulation at the many intraplate seamounts and small volcanic cones that erupt only rarely, or are monogenetic. At low magma supply rates these volcanoes should not have a shallow magma reservoir as a heat source for sustained hydrothermal activity (Clague and Dixon, 2000). A single submarine eruption can result in residual hydrothermal activity due to cooling and degassing (Santana-Casiano et al., 2016), but duration and implications of such activity remain to be explored. What is the thermal footprint of temporary fluid circulation on the seafloor? Can fluid circulation persist long enough for chemoautotrophic communities to develop, and are these common occurrences? These questions are difficult to address, largely because few deep-sea volcanoes have been thoroughly explored. Moreover, traces of previous hydrothermal activity are quickly buried by sediment, and any precipitated sulfide minerals and structures from hydrothermal flow will quickly oxidize and collapse. Any such discovery is rare. In this study, we provide evidence for waning Holocene hydrothermal activity at a Cretaceous seamount located near the Canary Islands that was likely caused by a small pulse of rejuvenated volcanism.

GEOLOGICAL BACKGROUND

The Canary Islands are part of an intraplate hotspot chain offshore NW Africa, with decreasing ages of seamounts and volcanic islands from east to west (**Figure 1A**). El Hierro, situated on ∼155 Ma old ocean crust, is the youngest island along the chain (1.1 Ma; Guillou et al., 1996) and is located near the present Canary hotspot (Geldmacher et al., 2005). The only historic eruption of El Hierro was submarine and occurred between 2011 and 2012 a few kilometers off the island's southern tip, with the shallowest peak shoaling to 89 m below sea level (Martí et al., 2013; Rivera et al., 2013). The new volcanic cone shows evidence for waning hydrothermal activity, given mostly by the expulsion of fluids rich in magmatic CO_2 (Santana-Casiano et al., 2016).

Henry Seamount, located 40 km southeast of El Hierro, is a volcanic edifice that rises ~700 m above ~3700 m deep ocean floor (Gee et al., 2001; **Figure 1B**). A reconnaissance dredging campaign over the seamount in 2005 yielded trachytic rocks that were dated by the $^{40}Ar/^{39}Ar$ method at 126 Ma, a barite block overgrown by a coral with a radiocarbon age of 41 ka, and shell fragments from vesicomyid clams, two of which gave radiocarbon ages of 3.4 and 18.6 ka, respectively (Klügel et al., 2011). Many trachyte fragments were barite-metasomatized. On the basis of these observations, these authors could show that Henry Seamount is an extinct early Cretaceous age volcano that is unrelated to the Canary hotspot (cf. Geldmacher et al., 2005) but shows low-temperature hydrothermal activity of Holocene age. They suggested that seawater infiltrated through basement outcrops of El Hierro's submarine flank, migrated and became heated within the oceanic crust to finally discharge at Henry Seamount. To test this hypothesis, we explored the seamount and the surrounding area in 2018 during R/V METEOR cruise M146 by high-resolution reflection seismics, heat flow determinations using a 6 m long probe, high-resolution hydroacoustic mapping with an autonomous underwater vehicle (AUV), TV-sled surveys, and sediment sampling with a gravity corer and a Van Veen grab.

METHODS

A description of the shipborne methods is given in Klügel and Shipboard Scientific Party (2018), and is summarized in the **Supplementary Material**.

Compositions of glasses from tephra and lava fragments were determined using a Cameca SX-100 electron microprobe (EMP) at the Department of Geosciences, University of Bremen. Glass was analyzed for major elements, S and Cl with an acceleration voltage of 15 kV, beam current of 40 nA, and a defocussed beam of 15 μm diameter. Peak counting times were 60 s for sulfur and chlorine and 10 s for most other elements; background counting times were half as long. Minerals and glasses from the Smithsonian Institution (Jarosewich et al., 1980) were used for calibration. Sulfur was calibrated using pyrite because peak analyses indicated similar maxima positions for sulfides, basaltic glass standards and samples, hence a predominance of S^{2-} speciation. Between two and seven EMP analyses were averaged for each glass sample. Analytical quality was monitored by repeated analyses of the glass standards VG-2 and VG-A99 (Smithsonian) and BHVO-2G and BCR-2G (USGS; Jochum et al., 2005) along with the samples. Precision of sulfur analyses was 3.5% for a concentration around 1400 ppm (VG-2), and 18% for a concentration around 150 ppm (VG-A99).

RESULTS

Seafloor Observations

A major discovery of cruise M146 was the widespread occurrence of dead vesicomyid clams in the summit area and the flanks of Henry Seamount. Locally, the seafloor is completely covered with shells, such that their distribution is very recognizable as prominent backscatter on high-resolution hydroacoustic maps (**Figures 1C,D**). Most clam shells belong to the genus *Abyssogena southwardae*, resembling those previously dredged at the seamount (Klügel et al., 2011). These clams live in symbiosis with sulfide-oxidizing bacteria at hydrothermal vents and cold seeps at >2980 water depth (Krylova et al., 2010), and have thus far not been reported elsewhere from the Canary Archipelago.

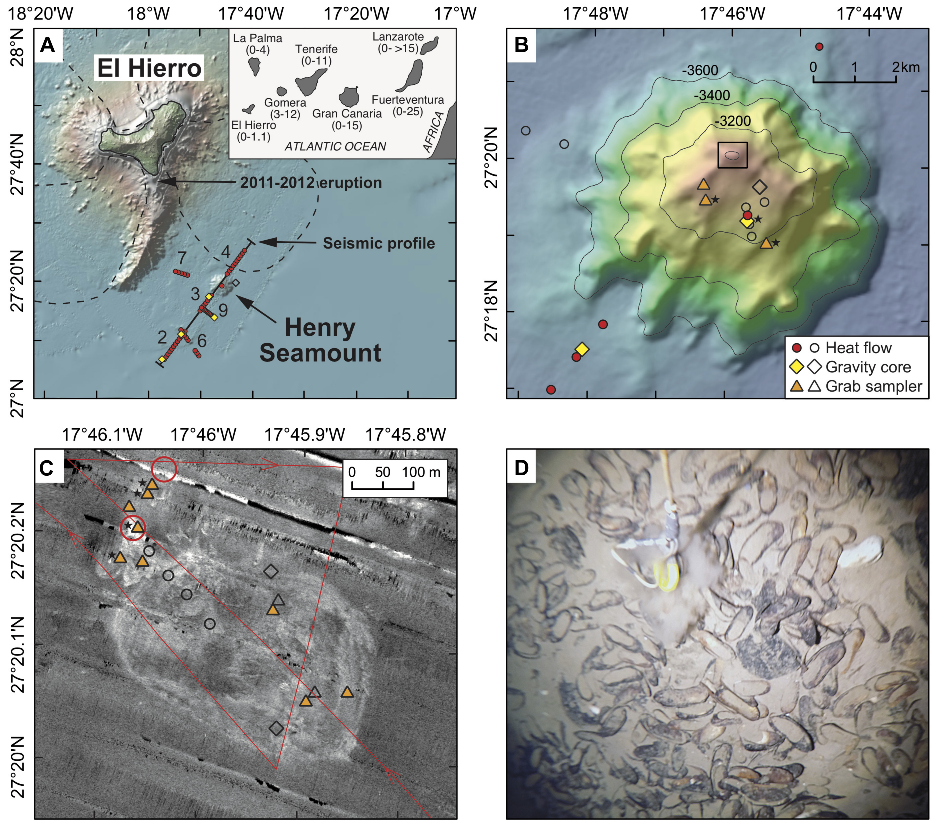

FIGURE 1 | (A) Location map of El Hierro and Henry Seamount, made with GeoMapApp (Ryan et al., 2009). Inset shows the Canary Islands, with numbers indicating the range of radiometric ages in Ma (from Geldmacher et al., 2005). Dashed lines outline landslide deposit boundaries after Gee et al. (2001). The line across Henry Seamount marks the seismic profile shown in **Figure 4**, red circles indicate positions of successful heat flow measurements, numbers identify heat flow profiles (e.g., "2" for profile HF1802, etc.), and diamonds indicate gravity corer sites. **(B)** Bathymetric map of Henry Seamount with 200 m contours, showing sites where sediment samples were taken and heat flow was determined. Open symbols indicate unsuccessful attempts, and stars mark sites where tephra was recovered. Rectangle outlines the area shown in panel **C**. **(C)** High-resolution backscatter map of Henry Seamount's summit area as obtained by AUV; symbols as in panel **B**. Red circles indicate localities of ORP anomalies shown in **Figure 2**; the corresponding TV-sled track is approximated by the red line. Areas with high backscatter (white-gray) indicate extensive coverage by clam shells or rock outcrops. **(D)** TV-sled photo from the summit area with vesicomyid clam shells up to 20 cm in size. Field of view is approximately 1 × 1 m.

A. southwardae has a wide distribution in the Atlantic including the Logatchev hydrothermal vent area, the Vema Fracture Zone, the Wideawake hydrothermal field, off Barbados, and offshore Virginia (Krylova et al., 2010). Preliminary radiocarbon ages for some of the recovered shells from Henry Seamount are consistent with the age range previously reported (Klügel et al., 2011). Many of the shells have a black coating of presumably manganese oxides, which is additional evidence that these vesicomyid communities are long dead. Living clams were not observed by the TV-sled, but grab samples showed some small-sized (<1 cm) chemosymbiotic thyasirid bivalves of the genus *Ochetoctena tomasi* with preserved inner soft tissues, which appear to have been alive prior to sampling (Krylova, personal communication). In the vicinity of some shell fields, the MAPRs on the TV-sled repeatedly recorded significant negative oxidation-reduction potential (ORP) anomalies a few meters above the seafloor (**Figure 2**). These anomalies are sensitive indicators for discharge of fluids with reduced chemical species (de Ronde et al., 2014; Baker et al., 2016), and indicate that hydrothermal flow at Henry Seamount is still ongoing. Associated thermal anomalies are lacking, probably because their amplitude is too small to be observed (cf. Baker et al., 2016).

Basaltic Samples

Six grab samples and one gravity core from the Henry Seamount summit area (**Figures 1B,C**) recovered basaltic tephra (heterolithologic coarse ash to small lapilli) and some dispersed basaltic rock fragments up to 4 cm in size. The tephra seems to be widespread on the plateau, with sample localities up to 2 km apart. It was covered by up to ~20 cm of pelagic sediment, and in some samples was weakly cemented. The mixture of different lithologies suggests that it has been reworked. Several tephra and rock fragment lithologies can be distinguished based on matrix and phenocryst assemblages. Glassy fragments with fresh sideromelane are prevalent; a few samples show incipient alteration on rims or cracks. Vesicularity varies from zero to about 50%; most vesicles are <1 mm in size. The dominant tephra lithology, denoted as ash type 1, consists of vesicular

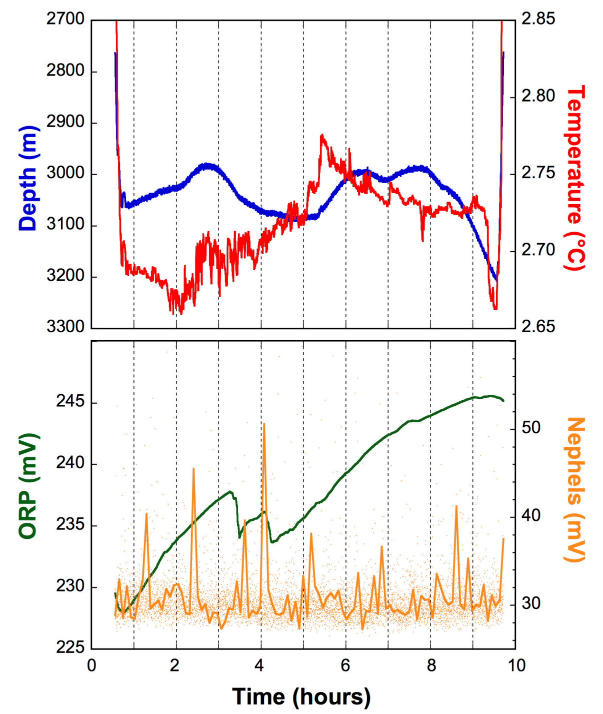

FIGURE 2 | Depth, temperature, oxidation-reduction potential (ORP), and backscatter (nephels) recorded during a TV-sled dive near the summit of Henry Seamount about 2 m above the seafloor. The two sharp ORP drops at ca. 03:20 and 04:10 h (cf. **Figure 1C**) indicate the presence of reduced species in the bottom water as is typical of discharged vent fluids; these anomalies were confirmed by subsequent TV-sled dives. The gradual increase following each ORP drop is caused by drifting electrode potential in response to changes in ambient parameters (Baker et al., 2016). The nephels curve (cubic spline fit) shows a number of peaks due to sediment particles raised up by the sled, but no significant anomaly. The temperature variations are partly correlated with depth and reflect the thermal gradient in the ocean as well as oceanographic effects such as bottom currents. Temperature spikes caused by hydrothermal plumes are of much lower amplitude (Baker et al., 2016) and are not recognized here.

sideromelane fragments with olivine phenocrysts ± plagioclase and rare clinopyroxene microlites (**Figure 3A**). Most fragments are angular and equant; flat bubble wall fragments similar to limu o Pele are rare. Type 1 and other glassy ash fragments closely resemble pyroclasts from deep-sea strombolian or hawaiian eruptions of volatile-rich magma (Clague et al., 2003; Eissen et al., 2003; Davis and Clague, 2006). By contrast, microlite-rich angular ash particles and larger rock fragments with flow texture appear to be derived from submarine lava flows.

The samples are dominantly alkalic to transitional basalts with major element compositions similar to subaerial and submarine whole-rock samples from El Hierro (**Figure 3B**). The sulfur contents of matrix and interstitial glasses from Henry Seamount (250–960 ppm) overlap with the range for glasses from submarine El Hierro samples (430–1480 ppm) but barely grade into that for subaerial glasses (<290 ppm). Glasses from ash type 1 consistently have the highest sulfur and lowest alkali and phosphorus contents of all Henry Seamount samples (**Figure 3**).

Heat Flow and Seismic Data

In order to establish the hydrogeological regime around Henry Seamount, we determined the heat flow distribution along lines co-located with seismic profiles, using a 6-m-long heat probe penetrating the sediment (**Figure 1A**). With one exception, all heat flow values are between 35 and 65 mW/m^2 with an average of 49 ± 7 mW/m^2 (±1 sigma), close to the value of 53 mW/m^2 predicted by conductive cooling of 155 Ma crust (Hasterok, 2013). Thus, there is no increased basal heat flow despite the proximity to the Canary hotspot. The highest value of 83 mW/m^2 was obtained at the summit region of Henry Seamount, where only one successful measurement could be achieved (**Figure 4B**). This value is subject to some uncertainty because the heat probe penetrated the sediment by only 2.5 m, thus the heat flow may be affected by local variation in sediment thickness, or erosional events. Conversely, purely conductive heat flow should decrease on top of a topographic high because isotherms would be spaced farther apart (Harris et al., 2004; **Figure 4C**). We cautiously suggest, therefore, that the elevated heat flow at the summit is real and that is related to the inferred hydrothermal activity.

A 50 km long SW-NE seismic and heat flow traverse across Henry Seamount (**Figure 4**) shows some heat flow variations, but no robust trend indicative of fluid recharge or discharge comparable to other hydrothermally active seamounts (Fisher and Harris, 2010). The most noticeable patterns is a weak gradual increase in heat flow toward the southwestern base of the seamount over a 5 km distance (**Figure 4B**). Overall, the seismic section reveals different sediment structures SW and NE of Henry Seamount, which is reflected in the heat flow patterns as well. For example, most heat flow values in the well-stratified sediments to the SW are slightly below the predicted value of 53 mW/m^2, whereas those to the NE are systematically higher (**Figure 4B**). In the SW, locally elevated heat flow values coincide with zones of seismic amplitude blanking (**Figure 4A**), i.e., reduction of the amplitude of seismic reflections caused, e.g., by the presence of gas hydrates (Lee and Dillon, 2001). A prominent blanking zone 10 km southwest of the seamount summit shows upward bending of adjacent reflectors, resembling doming linked to deeper magmatic intrusions and related hydrothermal activity (Berndt et al., 2016; Medialdea et al., 2017). This feature seems to be rather old because the overlying reflectors are not bent; it is also not accompanied by a heat flow anomaly (**Figure 4B**). The sediments to the NE of the seamount are characterized by strong reflectors in the upper 100 ms two-way travel time (TWT) with a hummocky surface, underlain by an almost transparent seismic unit (**Figure 4A**). This is indicative of mass transport deposits, and coincides with the extent of the >175 ka San Andres slump identified by Gee et al. (2001; **Figure 1A**).

DISCUSSION

Origin of Basaltic Samples

The recovery of fresh basaltic samples on a Cretaceous volcano raises the question whether this material originates from Henry Seamount itself, or from an adjacent volcano, with El Hierro

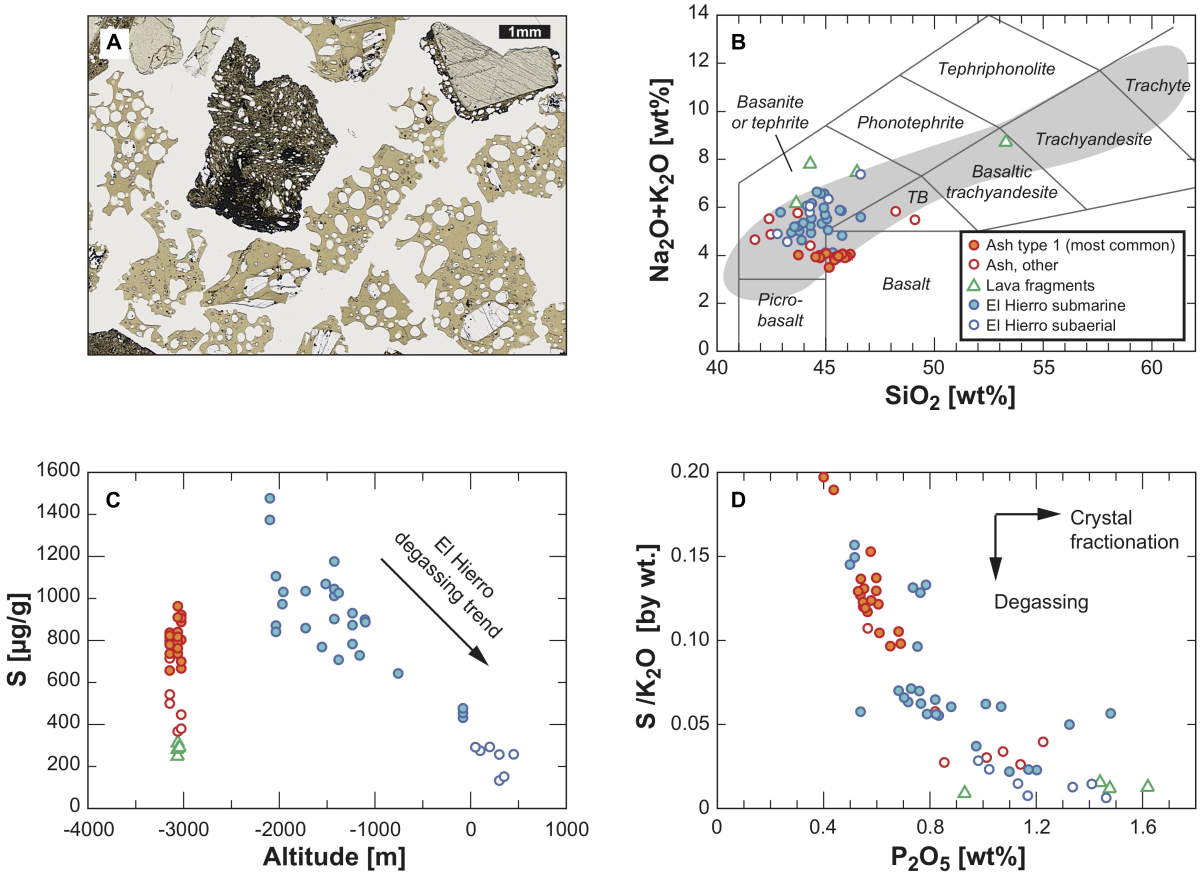

FIGURE 3 | (A) Microphotograph of glassy basaltic ash (sample 22841-1A, >0.5 mm sieve fraction) from Henry Seamount; note the lack of palagonitization and small vesicle diameters. Type 1 ash is dominated by fresh glass with olivine phenocrysts and few microlites. **(B)** Total alkalis versus silica (TAS) diagram of matrix and interstitial glasses from Henry Seamount samples, compared to matrix glasses from submarine samples (Stroncik et al., 2009; Longpré et al., 2014) and subaerial samples (this study) from El Hierro. The compositions overlap with those of whole-rock samples from El Hierro (gray field based on data from Pellicer, 1979; Carracedo et al., 2001; Stroncik et al., 2009; Day et al., 2010; Klügel et al., 2011). **(C)** Sulfur contents of matrix and interstitial glasses from Henry Seamount and from submarine and subaerial El Hierro samples (including data from Stroncik et al., 2009). The good correlation between sample altitude and S content of the El Hierro glasses indicates strong pressure control on sulfur degassing. **(D)** The S/K_2O versus P_2O_5 diagram shows that type 1 ash includes the least degassed samples, and that degassing is accompanied by crystal fractionation (Wallace and Edmonds, 2011).

being the only plausible source. For type 1 ash, an origin from El Hierro is unlikely for two main reasons. Firstly, the ash layer was found only on top of Henry Seamount but not in gravity cores in its vicinity (**Figure 1**), as would be expected if the ash represented a fallout or a mass flow deposit from El Hierro. Secondly, sulfur concentrations in type 1 ash glass are significantly higher than in subaerial or shallow submarine glasses from El Hierro. Sulfur contents strongly depend on melt degassing (Wallace and Edmonds, 2011), and for El Hierro correlate well with eruption depth (**Figure 3C**). Although S concentrations in Henry Seamount samples are below the El Hierro trend, which extrapolates to >1600 ppm at 3000 m depth, a plot of S/K_2O versus K_2O or P_2O_5 shows that type 1 ash glass is actually the least degassed, consistent with a deep submarine origin (**Figure 3D**). This plot discriminates between crystal fractionation and degassing processes, because S, K, and P are incompatible and maintain their ratios during mantle melting and crystallization (Wallace and Edmonds, 2011).

In contrast to type 1 ash, other basaltic samples from Henry Seamount appear to be more degassed than expected for a 3000 m water depth (**Figures 3C,D**). Glassy lava fragments have S and S/K_2O values similar to subaerial samples, which however does not rule out a submarine origin (cf. Davis et al., 1991). If derived from El Hierro, it is not clear how the dense fragments could have been transported to the top of Henry Seamount. Relocation by submarine mass flows appears unlikely. El Hierro's last giant flank collapse toward the southeast occurred at ca. 145 ka (Gee et al., 2001), thus the presence of fresh fragments >600 m above the adjacent seafloor can hardly be reconciled with this event.

Evidence for Rejuvenated Volcanism

The combined data strongly suggest that type 1 ash, and probably most other basaltic samples as well, originated from Henry Seamount. The age of the samples is not known, but the freshness of the glass and very limited vesicle fillings clearly exclude a genetic relation to the 126 Ma trachytes from

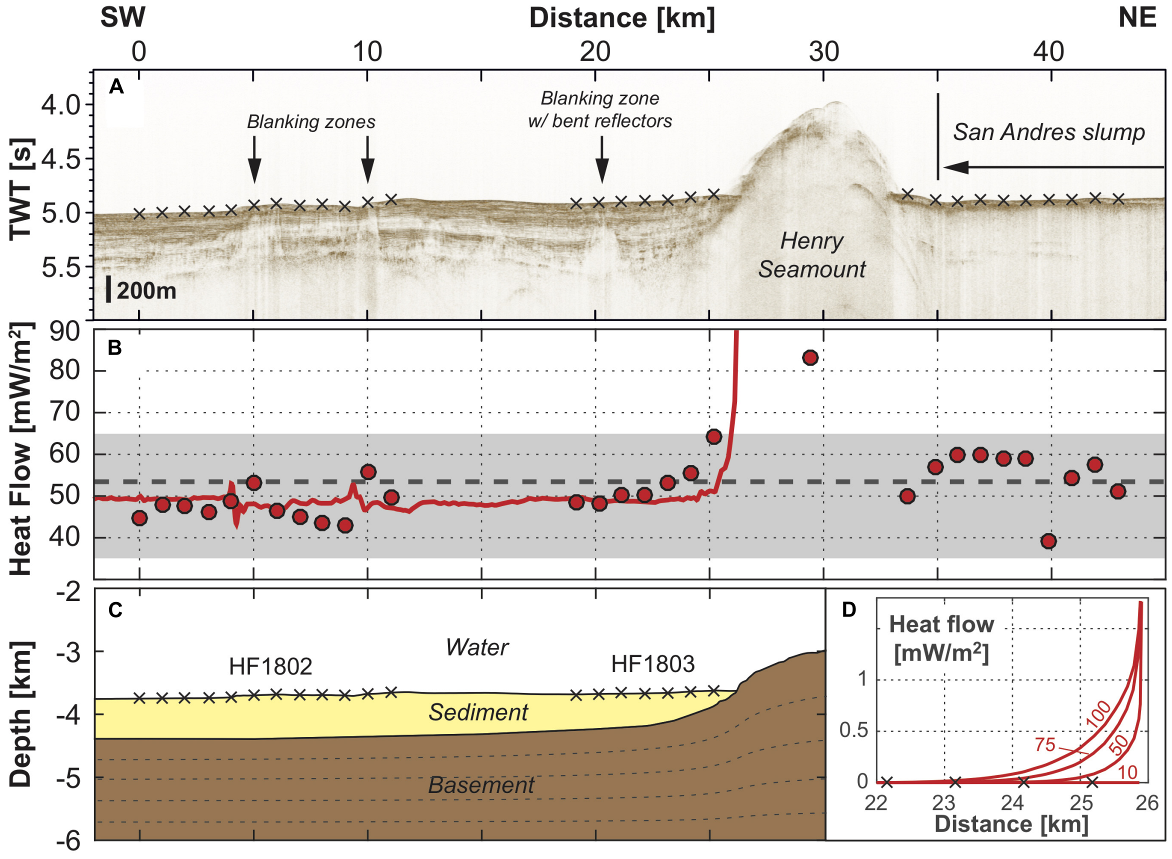

FIGURE 4 | (A) Southwest-northeast traverse across Henry Seamount as indicated in **Figure 1A**, showing the reflection seismic profile (vertical exaggeration 6×) and locations for heat flow measurements (crosses). The seismic data reveal several blanking zones, which may reflect the presence of gas hydrates (Lee and Dillon, 2001) or hydrothermal alteration of sediments by fluid circulation (Caratori Tontini et al., 2019). Boundary of the San Andres slump deposits after Gee et al. (2001). **(B)** Heat flows (red circles) determined along the seismic profile; the range for all other heat flow values near Henry Seamount (**Figure 1A**) is marked by gray shading. Except for a single value obtained near the summit, heat flow values cluster around the predicted lithospheric heat flow for 155 Ma old crust (dashed gray line; Hasterok, 2013). The solid red line shows the predicted conductive surface heat flow for the basal heating model shown in Panel **C**. **(C)** Geometry and parameters of the two-dimensional model used to simulate the surface heat flow southwest of Henry Seamount (see **Supplementary Material** for details of the calculations). Dashed lines symbolize isotherms; HF1802 and HF1803 are heat flow profiles. **(D)** Calculated seafloor heat flow at the southwestern base of the seamount for conductive cooling of a hypothetical cylindrical intrusion (see **Supplementary Material** for model details). Distance refers to the profile in panel **A**, numbers at calculated curves indicate intrusion age in ka, stars mark the heat probe locations of profile HF1803.

the seamount (Klügel et al., 2011). By comparison to 0.12–0.65 Ma glassy mid-ocean ridge basalts that show incipient palagonitization (Schramm et al., 2005), the unpalagonitized glassy samples are likely contemporaneous with the subaerial volcanic activity at El Hierro (<1.1 Ma; Guillou et al., 1996). The samples could be as young as the spatially associated clam shells and hydrothermal precipitates, i.e., a few ka to some tens of ka (Klügel et al., 2011). This would be consistent with <20 cm sediment coverage of ash observed in gravity core and grab samples, assuming a sedimentation rate of <7 cm/ka (Gee et al., 2001). In any case, the presence of fresh type 1 ash on top of Henry Seamount provides compelling evidence for one or more relatively recent eruptions of this otherwise Cretaceous volcano.

The limited recovery of ash in grab samples suggests one or more explosive low-volume eruptions, which may have produced a small vent with some tephra and little or no lava, rather than a significant volcanic cone. Such low-volume deposits can be difficult to identify in the bathymetric data or by TV-sled, in particular when draped by sediment, or covered by benthic communities. This may explain why our bathymetric data do not indicate an obvious crater or volcanic cone. Despite the limited eruption volume inferred, the difficulty of sediment penetration by gravity core and heat probe in the summit region (**Figure 1C**) suggests that the sandy ash layer has considerable thickness in some places.

The cause for rejuvenated volcanism may be related to the large extent of the melting anomaly beneath the Canary hotspot combined with plate motion (Geldmacher et al., 2005). That is, considering that there was Holocene volcanic activity across the entire archipelago, from Lanzarote in the east to the youngest islands La Palma and El Hierro in the west, there is little reason why one or more eruptions should not occur 40 km southeast of El Hierro. Some of the magma produced at the active end of the hotspot chain, which is not far from Henry Seamount, may have passed through a lithospheric region that was modified by the Cretaceous volcanism. Metasomatized mantle and mechanically weak zones may have focused further magma ascent, which eventually led to eruption just at the former volcano.

Heat Flow Modeling

We now turn our attention as to what caused the observed heat flow to increase by 16 mW/m^2 toward the southwestern base of Henry Seamount (**Figure 4B**). Plausible scenarios include (i) decreasing sediment thickness and thermal refraction, (ii) cooling of a magmatic intrusion within the seamount, or (iii) advective heat transport by hydrothermal circulation. To assess the influence of sediment thinning close to the seamount (i), we set up a steady-state conductive finite element model with axial symmetry and the seamount center as midpoint (**Figure 4C**); see the **Supplementary Material** for details of the calculations. The modeled surface heat flow is almost constant along the profile, and sharply increases toward the seamount flank (**Figure 4B**). However, the observed heat flow increase near the flank is well above the predicted increase for any realistic values of the model parameters. This shows that the thinning of the sediments cannot account for our observations and therefore, another heat source must be involved.

A second numerical simulation tested if conductive cooling of a hypothetical vertical intrusion in the center of the seamount could produce the observed heat flow increase (ii). We chose a vertical cylindrical intrusive body with a diameter of 100 m and initial temperature of 1200°C, extending from the top of the seamount downward (see **Supplementary Material**). This intrusion shape is not meant to imitate a natural basaltic intrusion, which would likely be a dike or sill of <100 m thickness, but rather to illustrate the thermal effect of an extreme scenario. The model results show that in this case the increase in surface heat flow at the closest heat probe location would reach only 0.4 mW/m^2 after 100 ka, well below the observed increase of 16 mW/m^2 (**Figure 4D**). It would be far less for a meter-thick basaltic dike. A significant increase in surface heat flow would result only if an intrusion were located close to the measured profile, which is not supported by our observations, or if advective heat transport played a major role.

Driver for Hydrothermal Activity

The results of our modeling suggest that the observed heat flow increase near the SW base of Henry Seamount cannot be explained by conductive cooling alone, but requires advective heat transport by hydrothermal circulation [model (iii) of above]. Compared to other hydrothermally active seamounts (Fisher and Harris, 2010), the heat flow increase is of small magnitude and lateral extent. This suggests a relatively recent origin and/or transient nature of hydrothermal circulation, with the sediments not having adapted to the thermal change at deeper levels. What is the driver for this flow? If the circulation represented ridge flank flow that is purely driven by seamount relief and basal heat from the cooling lithosphere (Harris et al., 2004; Fisher and Wheat, 2010), then it should have lasted for a long time and still persist, as there is no obvious reason for flow rates to decrease. This would not explain why the chemosynthetic communities are mostly extinct and manifested as shell graveyards, and why obtained ages for all samples related to hydrothermal activity are <41 ka (Klügel et al., 2011). Long-term basal heat from the nearby Canary hotspot cannot play a role for the same reason; in addition, our data do not show increased basal heat flow (**Figure 4B**). It is possible that relief-driven circulation plays a subordinate role at Henry Seamount, but its relative effect cannot be assessed from our limited data.

Our heat flow data and observed manifestations of hydrothermal discharge at the top of Henry Seamount are best explained by a scenario involving ephemeral periods of hydrothermal circulation. We propose that circulation was initiated, and is still driven, by weak pulses of rejuvenated volcanic activity that also produced the basaltic samples. The initial hydrothermal fluids probably were hot and sulfide-bearing, providing habitats for sulfur-oxidizing metabolisms and vesicomyids at the discharge sites. The decay of magmatic heat soon resulted in waning hydrothermal flow and extinction of the chemosynthetic communities; eventually a new magmatic event brought another heat pulse and renewed hydrothermalism. An ephemeral character of hydrothermal flow at Henry Seamount could also explain the low amount of hydrothermal deposits observed; thus far only local barite precipitates were found (Klügel et al., 2011). Considering the presumably low erupted volume at Henry Seamount and overall similarity to El Hierro lavas, the existence of a crustal magma reservoir is highly unlikely (cf. Klügel et al., 2015), hence, the magmatic heat must have been delivered from the volcanic deposits and/or a shallow dike. This scenario has some resemblance to the weak diffuse hydrothermal activity observed at the Lilliput field, southern Mid-Atlantic Ridge, which is thought to have resulted from a single diking event (Haase et al., 2009).

If the development of hydrothermal circulation and chemosynthetic communities at Henry Seamount was indeed a consequence of single magmatic pulses, then similar scenarios might be envisaged for many other volcanic seamounts in the deep ocean basins. Whether they are monogenetic or form by a succession of eruptions over a long period of time, each eruption has the potential to drive ephemeral hydrothermal activity (e.g., Medialdea et al., 2017; German et al., 2020), which may provide habitats for chemosynthetic communities. The same holds for the submarine flanks of volcanic islands that are often scattered with presumably monogenetic volcanic cones (e.g., Santana-Casiano et al., 2016). Detection of short-lived hydrothermal circulation is challenging, however, because the response of surface heat flow is weak and the sites may become increasingly blanketed by sediment after cessation of activity. Moreover, deep-sea chemosynthetic communities are not well preserved in the geological record (Krylova et al., 2010). As exploration of the deep sea is still very limited, Henry Seamount may be a rare example of a common feature rather than a special case.

DATA AVAILABILITY STATEMENT

Readers can access our data on the Pangaea data base (https://doi.pangaea.de/10.1594/PANGAEA.913552), and the report of cruise M146 is available at https://doi.org/10.2312/cr_m146.

AUTHOR CONTRIBUTIONS

AK, HV, SK, and MR conceived the project. AK investigated the tephra samples and wrote most of the text. HV and NK collected and processed the heat flow data. SK and KFL collected and processed the seismic data. PW and MR collected and processed the multibeam data. All authors were actively involved in the discussion, interpretation of the data, and preparation of the manuscript.

FUNDING

Our research was funded by the Deutsche Forschungsgemeinschaft (DFG, grant KL1313/18-1), and MR was funded by the DFG under Germany's Excellence Strategy – EXC-2077 – 390741603.

ACKNOWLEDGMENTS

We are grateful to Captain R. Hammacher, the crew and the shipboard scientific party of METEOR cruise M146 for excellent work, and the Leitstelle Deutsche Forschungsschiffe for overall support. We thank C. Hübscher (University of Hamburg) for kindly loaning us a sparker array on short notice, S. Walker for providing MAPRs and advice, and G. Bohrmann and E. Krylova for helpful discussions. The constructive comments by R. Harris, C. de Ronde, and the reviewers are appreciated and improved the manuscript.

SUPPLEMENTARY MATERIAL

The Supplementary Material for this article can be found online at: https://www.frontiersin.org/articles/10.3389/fmars.2020.584571/full#supplementary-material

Supplementary Text | Methods and parameters for the numerical modeling, and shipborne methods.

REFERENCES

Baker, E. T., Resing, J. A., Haymon, R. M., Tunnicliffe, V., Lavelle, J. W., Martinez, F., et al. (2016). How many vent fields? New estimates of vent field populations on ocean ridges from precise mapping of hydrothermal discharge locations. *Earth Planet. Sci. Lett.* 449, 186–196. doi: 10.1016/j.epsl.2016.05.031

Berndt, C., Hensen, C., Mortera-Gutierrez, C., Sarkar, S., Geilert, S., Schmidt, M., et al. (2016). Rifting under steam - How rift magmatism triggers methane venting from sedimentary basins. *Geology* 44, 767–770. doi: 10.1130/G38049.1

Butterfield, D. A. (2000). "Deep ocean hydrothermal vents," in *The Encyclopedia of Volcanoes (First Edition)*, ed. H. Sigurdsson (Amsterdam: Academic Press), 857–875.

Caratori Tontini, F., Tivey, M. A., de Ronde, C. E. J., and Humphris, S. E. (2019). Heat flow and near-seafloor magnetic anomalies highlight hydrothermal circulation at brothers Volcano Caldera, Southern Kermadec Arc, New Zealand. *Geophys. Res. Lett.* 46, 8252–8260. doi: 10.1029/2019GL083517

Carracedo, J. C., Badiola, E. R., Guillou, H., de La Nuez, J., and Pérez Torrado, F. J. (2001). Geology and volcanology of La Palma and El Hierro, Western Canaries. *Estudios Geol.* 57, 175–273.

Clague, D. A., Batiza, R., Head, J. W. III, and Davis, A. S. (2003). "Pyroclastic and hydroclastic deposits on Loihi Seamount, Hawaii," in *Explosive Subaqueous Volcanism*, eds J. D. L. White, J. L. Smellie, and D. A. Clague (Washington DC: American Geophysical Union), 73–95. doi: 10.1029/140gm05

Clague, D. A., and Dixon, J. E. (2000). Extrinsic controls on the evolution of Hawaiian ocean island volcanoes. *Geochem. Geophys. Geosyst.* 1:GC000023. doi: 10.1029/1999GC000023

Davis, A. S., and Clague, D. A. (2006). Volcaniclastic deposits from the North Arch volcanic field, Hawaii: explosive fragmentation of alkalic lava at abyssal depths. *Bull. Volcanol.* 68, 294–307. doi: 10.1007/s00445-005-0008-7

Davis, A. S., Clague, D. A., Schulz, M. S., and Hein, J. R. (1991). Low sulfur content in submarine lavas: an unreliable indicator of subaerial eruption. *Geology* 19, 750–753. doi: 10.1130/0091-7613(1991)019<0750:lscisl>2.3.co;2

Day, J. M. D., Pearson, D. G., Macpherson, C. G., Lowry, D., and Carracedo, J. C. (2010). Evidence for distinct proportions of subducted oceanic crust and lithosphere in HIMU-type mantle beneath El Hierro and La Palma, Canary Islands. *Geochim. Cosmochim. Acta* 74, 6565–6589. doi: 10.1016/j.gca.2010.08.021

de Ronde, C. E. J., and Stucker, V. K. (2015). "Seafloor hydrothermal venting at volcanic arcs and backarcs," in *The Encyclopedia of Volcanoes (Second Edition)*, ed. H. Sigurdsson (Amsterdam: Academic Press), 823–849. doi: 10.1016/b978-0-12-385938-9.00047-x

de Ronde, C. E. J., Walker, S. L., Ditchburn, R. G., Tontini, F. C., Hannington, M. D., Merle, S. G., et al. (2014). The anatomy of a buried submarine hydrothermal system, Clark Volcano, Kermadec Arc, New Zealand. *Econom. Geol.* 109, 2261–2292. doi: 10.2113/econgeo.109.8.2261

Eissen, J.-P., Fouquet, Y., Hardy, D., and Ondréas, H. (2003). "Recent MORB Volcaniclastic explosive deposits formed between 500 and 1750 m.b.s.l. on the axis of the Mid-Atlantic Ridge, south of the Azores," in *Explosive Subaqueous Volcanism*, eds J. D. L. White, J. L. Smellie, and D. A. Clague (Washington DC: American Geophysical Union), 143–166. doi: 10.1029/140gm09

Fisher, A. T., Davis, E. E., Hutnack, M., Spiess, V., Zuehlsdorff, L., Cherkaoui, A., et al. (2003). Hydrothermal recharge and discharge across 50 km guided by seamounts on a young ridge flank. *Nature* 421, 618–621. doi: 10.1038/nature01352

Fisher, A. T., and Harris, R. N. (2010). Using seafloor heat flow as a tracer to map subseafloor fluid flow in the ocean crust. *Geofluids* 10, 142–160. doi: 10.1111/j.1468-8123.2009.00274.x

Fisher, A. T., and Wheat, C. G. (2010). Seamounts as conduits for massive fluid, heat, and solute fluxes on Ridge Flanks. *Oceanography* 23, 74–87. doi: 10.5670/oceanog.2010.63

Gee, M. J. R., Watts, A. B., Masson, D. G., and Mitchell, N. C. (2001). Landslides and the evolution of El Hierro in the Canary Islands. *Mar. Geol.* 177, 271–293. doi: 10.1016/s0025-3227(01)00153-0

Geldmacher, J., Hoernle, K., Bogaard, P. V. D., Duggen, S., and Werner, R. (2005). New 40Ar/39Ar age and geochemical data from seamounts in the Canary and Madeira volcanic provinces: support for the mantle plume hypothesis. *Earth Planet. Sci. Lett.* 237, 85–101. doi: 10.1016/j.epsl.2005.04.037

German, C. R., Resing, J. A., Xu, G., Yeo, I. A., Walker, S. L., Devey, C. W., et al. (2020). Hydrothermal activity and seismicity at teahitia seamount: reactivation of the society Islands hotspot? *Front. Mar. Sci.* 7:73. doi: 10.3389/fmars.2020.00073

Guillou, H., Carracedo, J. C., Perez Torrado, F. J., and Rodrıguez Badiola, E. (1996). K–Ar ages and magnetic stratigraphy of a hotspot-induced, fast grown oceanic island: El Hierro, Canary Islands. *J. Volcanol. Geotherm. Res.* 73, 141–155. doi: 10.1016/0377-0273(96)00021-2

Haase, K. M., Koschinsky, A., Petersen, S., Devey, C. W., German, C., Lackschewitz, K. S., et al. (2009). Diking, young volcanism and diffuse hydrothermal activity on the southern Mid-Atlantic Ridge: the Lilliput field at 9∘33'S. *Mar. Geol.* 266, 52–64. doi: 10.1016/j.margeo.2009.07.012

Harris, R. N., Fisher, A. T., and Chapman, D. S. (2004). Fluid flow through seamounts and implications for global mass fluxes. *Geology* 32, 725–728. doi: 10.1130/g20387.1

Hasterok, D. (2013). A heat flow based cooling model for tectonic plates. *Earth Planet. Sci. Lett.* 361, 34–43. doi: 10.1016/j.epsl.2012.10.036

Hillier, J. K., and Watts, A. (2007). Global distribution of seamounts from ship-track bathymetry data. *Geophys. Res. Lett.* 34:L13304. doi: 10.1029/2007GL029874

Jarosewich, E. J., Nelen, J. A., and Norberg, J. A. (1980). Reference samples for electron microprobe analysis. *Geostand. Newslett.* 44, 257–258.

Jochum, K. P., Willbold, M., Raczek, I., Stoll, B., and Herwig, K. (2005). Chemical characterisation of the USGS reference glasses GSA-1G, GSC-1G, GSD-1G, GSE-1G, BCR-2G, BHVO-2G and BIR-1G Using EPMA, ID-TIMS, ID-ICP-MS and LA-ICP-MS. *Geostand. Geoanal. Res.* 29, 285–302. doi: 10.1111/j.1751-908x.2005.tb00901.x

Klügel, A., Fraile Nuez, E., and Shipboard Scientific Party (2018). *Henry Seamount Seepage Exploration (HESSE).* METEOR-Berichte, Cruise No. M146. Bonn: Gutachterpanel Forschungsschiffe.

Klügel, A., Hansteen, T. H., Bogaard, P. V. D., Strauss, H., and Hauff, F. (2011). Holocene fluid venting at an extinct Cretaceous seamount, Canary archipelago. *Geology* 39, 855–858. doi: 10.1130/g32006.1

Klügel, A., Longpré, M.-A., García-Cañada, L., and Stix, J. (2015). Deep intrusions, lateral magma transport and related uplift at ocean island volcanoes. *Earth Planet. Sci. Lett.* 431, 140–149. doi: 10.1016/j.epsl.2015.09.031

Krylova, E. M., Sahling, H., and Janssen, R. (2010). Abyssogena: a new genus of the family Vesicomyidae (bivalvia) from deep-water vents and seeps. *J. Molluscan Stud.* 76, 107–132. doi: 10.1093/mollus/eyp052

Lee, M. W., and Dillon, W. P. (2001). Amplitude blanking related to the pore-filling of gas hydrate in sediments. *Mar. Geophys. Res.* 22, 101–109. doi: 10.1023/A:1010371308699

Longpré, M. A., Klügel, A., Diehl, A., and Stix, J. (2014). Mixing in mantle magma reservoirs prior to and during the 2011–2012 eruption at El Hierro, Canary Islands. *Geology* 42, 315–318. doi: 10.1130/G35165.1

Martí, J., Pinel, V., López, C., Geyer, A., Abella, R., Tárraga, M., et al. (2013). Causes and mechanisms of the 2011–2012 El Hierro (Canary Islands) submarine eruption. *J. Geophys. Res.* 118, 1–17. doi: 10.1002/jgrb.50087

Medialdea, T., Somoza, L., González, F. J., Vázquez, J. T., de Ignacio, C., Sumino, H., et al. (2017). Evidence of a modern deep water magmatic hydrothermal system in the Canary Basin (eastern central Atlantic Ocean). *Geochem. Geophys. Geosyst.* 18, 3138–3164. doi: 10.1002/2017gc006889

Pellicer, J. M. (1979). Estudio geoquìmico del vulcanismo de la isla del Hierro, Archipieìlago Canario. *Estudios Geol.* 35, 15–29.

Rivera, J., Lastras, G., Canals, M., Acosta, J., Arrese, B., Hermida, N., et al. (2013). Construction of an oceanic island: insights from the El Hierro (Canary Islands) 2011-2012 submarine volcanic eruption. *Geology* 41, 355–358. doi: 10.1130/G33863.1

Ryan, W. B. F., Carbotte, S. M., Coplan, J., O'Hara, S., Melkonian, A., Arko, R., et al. (2009). Global multi-resolution topography (GMRT) synthesis data set. *Geochem. Geophys. Geosyst.* 10:Q03014. doi: 10.1029/2008GC002332

Sakai, H., Tsubota, H., Nakai, T., Ishibashi, J., Akagi, T., Gamo, T., et al. (1987). Hydrothermal activity on the summit of Loihi Seamount, Hawaii. *Geochem. J.* 21, 11–21. doi: 10.2343/geochemj.21.11

Santana-Casiano, J. M., Fraile-Nuez, E., Gonzaìlez-Daìvila, M., Baker, E. T., Resing, J. A., and Walker, S. L. (2016). Significant discharge of CO2 from hydrothermalism associated with the submarine volcano of El Hierro Island. *Sci. Rep.* 6:25686. doi: 10.1038/srep25686

Schramm, B., Devey, C. W., Gillis, K. M., and Lackschewitz, K. (2005). Quantitative assessment of chemical and mineralogical changes due to progressive low-temperature alteration of East Pacific Rise basalts from 0 to 9 Ma. *Chem. Geol.* 218, 281–313. doi: 10.1016/j.chemgeo.2005.01.011

Staudigel, H., and Clague, D. A. (2010). The geological history of deep-sea volcanoes. *Oceanography* 23, 58–71. doi: 10.5670/oceanog.2010.62

Staudigel, H., Hart, S. R., Koppers, A. A. P., Constable, C., Workman, R., Kurz, M., et al. (2004). Hydrothermal venting at Vailulu'u Seamount: the smoking end of the Samoan chain. *Geochem. Geophys. Geosyst.* 5:Q02003. doi: 10.1029/2003GC000626

Stroncik, N. A., Klügel, A., and Hansteen, T. H. (2009). The magmatic plumbing system beneath El Hierro (Canary Islands): constraints from phenocrysts and naturally quenched basaltic glasses in submarine rocks. *Contrib. Mineral. Petrol.* 157, 593–607. doi: 10.1007/s00410-008-0354-5

Villinger, H., Grevemeyer, I., Kaul, N., Hauschild, J., and Pfender, M. (2002). Hydrothermal heat flux through aged oceanic crust: where does the heat escape? *Earth Planet. Sci. Lett.* 202, 159–170. doi: 10.1016/s0012-821x(02)00759-8

Villinger, H. W., Pichler, T., Kaul, N., Stephan, S., Pälike, H., and Stephan, F. (2017). Formation of hydrothermal pits and the role of seamounts in the Guatemala Basin (Equatorial East Pacific) from heat flow, seismic, and core studies. *Geochem. Geophys. Geosyst.* 18, 369–383. doi: 10.1002/2016GC006665

Wallace, P. J., and Edmonds, M. (2011). "The sulfur budget in magmas: evidence from melt inclusions, submarine glasses, and volcanic gas emissions," in *Reviews in Mineralogy Vol. 73: Sulfur in Magmas and Melts*, eds H. Behrens and J. D. Webster (Washington DC: Mineralogical Society of America), 215–246. doi: 10.2138/rmg.2011.73.8

Wessel, P. (2001). Global distribution of seamounts inferred from gridded Geosat/ERS-1 altimetry. *J. Geophys. Res.* 106, 19431–19441. doi: 10.1029/2000jb000083

Conflict of Interest: The authors declare that the research was conducted in the absence of any commercial or financial relationships that could be construed as a potential conflict of interest.